Antibody to Langerin/CD207 localizes large numbers of CD8α^+ dendritic cells to the marginal zone of mouse spleen

Juliana Idoyaga, Nao Suda, Koji Suda, Chae Gyu Park, and Ralph M. Steinman[1]

Laboratory of Cellular Physiology and Immunology and Chris Browne Center for Immunology and Immune Diseases, The Rockefeller University, 1230 York Avenue, New York, NY 10065

Contributed by Ralph M. Steinman, December 3, 2008 (sent for review November 3, 2008)

Dendritic cells (DCs) are strategically positioned to take up antigens and initiate adaptive immunity. One DC subset expresses CD8$\alpha\alpha$ in mice and is specialized to capture dying cells and process antigens for MHC class I "cross-presentation." Because CD8$^+$ DCs also express DEC205/CD205, which is localized to splenic T cell regions, it is thought that CD8$^+$ DCs also are restricted to T zones. Here, we used a new antibody to Langerin/CD207, which colabels isolated CD8$^+$ CD205$^+$ DCs, to immunolabel spleen sections. The mAb labeled discrete cells with high levels of CD11c and CD8. Surprisingly most CD207$^+$ profiles were in marginal zones surrounding splenic white pulp nodules, and only smaller numbers were in T cell areas, where CD205 colabeling was noted. Despite a marginal zone location, CD207$^+$ DCs lacked identifying molecules for 3 different types of macrophages, localized in proximity and, in contrast to macrophages, marginal zone DCs were poor scavengers of soluble and particulate substrates. After stimulation with microbial agonists, Langerin expression disappeared from the marginal zone at 6–12 h, but was greatly expanded in the T cell areas, and by 24–48 h, Langerin expression disappeared. Therefore, anti-Langerin antibodies localize a majority of CD8$^+$ DCs to non-T cell regions of mouse spleen, where they are distinct from adjacent macrophages.

To induce adaptive immunity, a critical event is the uptake and presentation of antigen by dendritic cells (DCs) to naïve T cells. DCs initiate protective responses to infection and vaccination, and they also maintain self-tolerance (1, 2). Several subsets of DCs exist in the steady state, and these can have distinct functions (3, 4). In spleen, the main immune organ used for studies of immunity in mice, 2 main subsets of classical DCs are distinguished. Although both express high CD11c integrin, one subset expresses CD8$\alpha\alpha$, a marker of unknown function, and the other lacks CD8 but often expresses CD4 (5). CD8$^+$ DCs are specialized to induce Th1 helper T cell development and to capture dying cells and cross-present antigens on MHC class I, whereas CD8$^-$ DCs elicit IL-4 and more efficiently form peptide MHC II complexes (6–11).

DC subsets differ in expression of antigen uptake receptors. CD8$^+$ DCs express higher levels of DEC205/CD205 (5, 12), recognized by the mAb NLDC-145 (13, 14), whereas CD8$^-$ DCs express DCIR2, recognized by 33D1 mAb (10). The capacity of DEC205 and DCIR2 to efficiently mediate antigen presentation in vivo can be demonstrated by injecting the corresponding anti-receptor mAbs engineered to deliver antigenic proteins (10, 15).

The anatomy of mouse spleen is highly organized. The white pulp (WP) contains T cells, located in periarterial lymphoid sheaths (PALS), and B cells, found in discrete follicles. A marginal zone (MZ) rich in marginal zone macrophages (MZMs) and marginal metallophillic macrophages (MMMs) surrounds each WP nodule. Surrounding the MZ is the red pulp (RP), rich in red pulp macrophages (RPMs) (16, 17). CD11c-rich DCs are prevalent in the MZ and PALS (18). The location of both subsets of classic DCs (CD8$^+$ and CD8$^-$) is defined by using mAbs against DEC205 and DCIR2 in spleen sections. DEC205 staining in mouse spleen is restricted to PALS (13, 19), whereas DCIR2 staining is restricted to the bridging region of the MZ (10). Consequently, it is widely accepted that splenic CD8$^+$ DCs are localized to DEC205-rich T cell areas (20–22).

We recently developed an IgG mAb to the extracellular domain of mouse Langerin/CD207 (23). In the spleen, this mAb identifies CD207 selectively in CD8$^+$ DCs, as also has been found with other approaches (12, 24). When anti-Langerin is engineered to deliver an antigen in vivo, it too mediates efficient presentation, both in peripheral lymph nodes and spleen (15). Here, we took advantage of the L31 anti-CD207 mAb to localize CD8$^+$ DCs in spleen sections. Unexpectedly, CD207$^+$ CD8$^+$ DCs were mainly localized to the MZ, with fewer cells in the RP and PALS. Langerin$^+$ cells lacked the major markers of 3 different groups of adjacent phagocytes, and despite their location, CD207$^+$ CD8$^+$ DCs only weakly cleared a variety of substrates from the blood.

Results

CD207, CD205, and CD8 Antibodies Colabel a DC Subset in Spleen Cell Suspensions. Previously, we reported that the L31 mAb against the extracellular domain of mouse Langerin/CD207 is able to label the CD8$^+$ DC subset in spleen cell suspensions from BALB/c and BALB/c × C57BL/6 F_1 mice, but poorly labels this subset in C57BL/6 mice (23). This labeling increases markedly after fixation and permeabilization, suggesting that Langerin is primarily intracellular in location. To simultaneously examine CD207 and CD205 expression on different cell types in mouse spleen, we used an 8-color flow cytometry strategy to distinguish DCs, monocytes, RPMs, and granulocytes [supporting information (SI) Fig. S1]. Classical DCs were identified by high CD11c integrin expression and, as expected, consisted of CD11b^{high} CD8$^-$ and CD11b^{low} CD8$^+$ subsets (Fig. S1) (12). Most of the CD8$^+$ cells expressed Langerin and DEC205 (Fig. 1*A*), confirming that these 2 antigen uptake receptors are primarily expressed on CD8$^+$ DCs, as described previously (12, 24).

We next considered RPMs, the macrophage population most easily identified by FACS. RPMs expressed high F4/80 and low CD11c and CD11b (Fig. S1) (25). RPMs failed to label for either CD207 or CD205 (Fig. 1*B Upper*), but stained strongly for mannose receptor/CD206 and CD68 (Fig. 1*B Lower*).

We also looked for Langerin in other nonlymphocyte populations (Fig. S1): plasmacytoid DCs (PDCA-1$^+$, B220$^+$, CD11c^{int}, CD11b^{low}), monocytes (CD11b$^+$, CD115$^+$ Ly6G$^-$), and granulocytes (CD11b$^+$ Ly6G$^+$). None of these populations

Author contributions: J.I. and R.M.S. designed research; J.I., N.S., and K.S. performed research; J.I. and C.G.P. contributed new reagents/analytic tools; J.I. and R.M.S. analyzed data; and J.I. and R.M.S. wrote the paper.

The authors declare no conflict of interest.

[1]To whom correspondence should be addressed. E-mail: steinma@mail.rockefeller.edu.

This article contains supporting information online at www.pnas.org/cgi/content/full/0812247106/DCSupplemental.

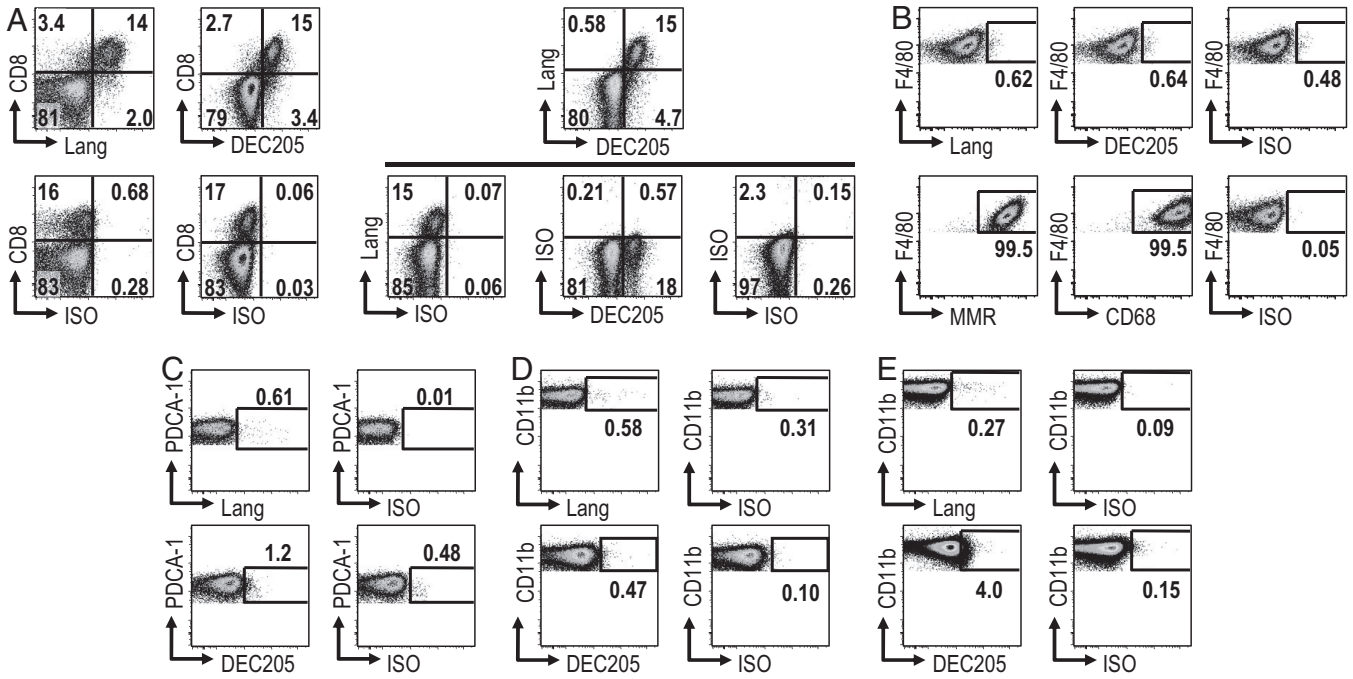

Fig. 1. L31 mAb specifically recognizes CD8$^+$ DCs. Fixed and permeabilized B cell depleted BALB/c splenocytes were analyzed by multicolor flow cytometry (Fig. S1). (*A*) Expression of Langerin, DEC205, and CD8 in CD11c high gated cells (Fig. S1, gate g). (*B*) RPMs (Fig. S1, gate j) were evaluated for Langerin, DEC205, MMR, and CD68. (*C–E*) Langerin and DEC205 expression was analyzed in (*C*) plasmacytoid DCs (Fig. S1, gate k), (*D*) monocytes (Fig S1, gate n), and (*E*) granulocytes (Fig. S1, gate l). One experiment representative of 3 is shown.

expressed significant Langerin, but granulocytes had low CD205 (Fig. 1 *C*, *D*, and *E*, respectively) (26). These data indicated that Langerin/CD207 and DEC205/CD205 should be suitable markers to localize CD8$^+$ DCs in sections of intact spleen.

Most Langerin$^+$ DCs Are in the Splenic MZ but Lack Macrophage Markers. CD8$^+$ DCs are thought to be restricted to the T cell area of spleen because these cells colabel for DEC205 in cell suspensions (10, 27), and DEC205 staining in tissue sections is limited to the PALS (13, 28). Surprisingly, CD207$^+$ cells were observed primarily in MZ, with some in RP and PALS (Fig. 2). In sections through WP regions containing B cell areas, Langerin$^+$ cells formed a ring around each WP nodule, separating the B cell area from F4/80$^+$ RPM (Fig. 2*A*). In sections containing T cell areas, Langerin$^+$ cells also were found in the PALS (29), but the dominant location was in the MZ surrounding rings of CD169$^+$ MMMs (Fig. 2*B*).

At higher power, CD207$^+$ DCs (Fig. 2 *C–G*, red) were distinct from, but interspersed with, SIGNR1/CD209b$^+$ MZMs (Fig. 2 *E* and *G*, blue), just internal to F4/80$^+$ RPM (Fig. 2 *C–E*), and surrounding CD169$^+$ MMMs (Fig. 2 *F* and *G*). Unexpectedly, then, most Langerin/CD207$^+$ DCs were localized to the splenic MZ, with smaller numbers in the RP and WP, but the cells were distinct from F4/80$^+$, SIGNR1$^+$, and CD169$^+$ macrophages.

Langerin$^+$ Cells in Spleen Sections Express High CD8 but Variable DEC205/CD205. To examine coexpression of Langerin with DC markers in spleen tissue sections, we first considered CD11c (Fig. 3*A*). Langerin$^+$ cells all colabeled for CD11c, both in the MZ (Fig. 3A *Upper*) and in the PALS (Fig. 3A *Lower*). Many CD11c^{high} cells lacked CD207 (Fig. 3*A*) and likely represent CD8$^-$ CD207$^-$ DCs.

When we double labeled for CD8, tight coexpression of CD8 (green) and CD207 (red) was readily evident in the MZ (Fig. 3*B Upper*), confirming the FACS data (Fig. 1*A Upper Left*). This double labeling was more difficult to discern in the PALS because of the numerous CD8$^+$ T cells there (Fig. 3*B Lower Right*).

DEC205 is not known to be present in the MZ, suggesting that the DEC205 noted by FACS on Langerin$^+$ cells (Fig. 1*A Upper*) was too scarce to be detected in sections. However, DEC205 was evident in PALS (Fig. 3*C*, red); there, staining for CD205 and CD207 showed that many DEC205$^+$ cells expressed Langerin (Fig. 3*C Bottom*). These results suggest that DEC205 expression on most isolated CD8$^+$ DCs by FACS is too low to visualize in sections with current methods, and that Langerin is a better marker for CD8$^+$ CD11c^{high} DCs.

Langerin$^+$ CD8α^+ DCs Poorly Take up Substrates Injected Intravenously. Large bloodborne particles (>75 kDa) are trapped in the splenic MZ (16), and only cells located in the RP and MZ have access to them. The localization of Langerin$^+$ cells in the splenic MZ prompted us to evaluate their ability to take up bloodborne particles. Mice were injected i.v. with different fluorescent labeled substances, and 30 min or 3 h later we analyzed uptake by flow cytometry. Large particles, like yellow-green polystyrene (YG-PS), soluble BSA, and killed *Escherichia coli* or *Staphylococcus aureus* Alexa 488 were taken up comparably by CD8$^+$ and CD8$^-$ DCs (Fig. 4). Nevertheless, only a small fraction (≈3–10%) of DCs were phagocytic and also took up small amounts, whereas most RPMs more actively took up all labeled substrates (Fig. 4).

Langerin$^+$ CD8α^+ MZ DCs Poorly Phagocytose Particles Injected Intravenously. To further identify cells taking up bloodborne particles, we looked in spleen sections for uptake of fluorescent YG-PS (Fig. 5 *A–C*), Alexa 488-*E. coli* (Fig. 5*D*), and Alexa 488-*S. aureus* (Fig. 5*E*) 30 min after i.v. inoculation. Sections allowed an examination of macrophages that were not readily released into cell suspensions. As illustrated for YG-PS in Fig. 5*A Upper*, bloodborne particles accumulated in cells of the MZ but not the WP. However, the vast majority of Langerin$^+$ cells

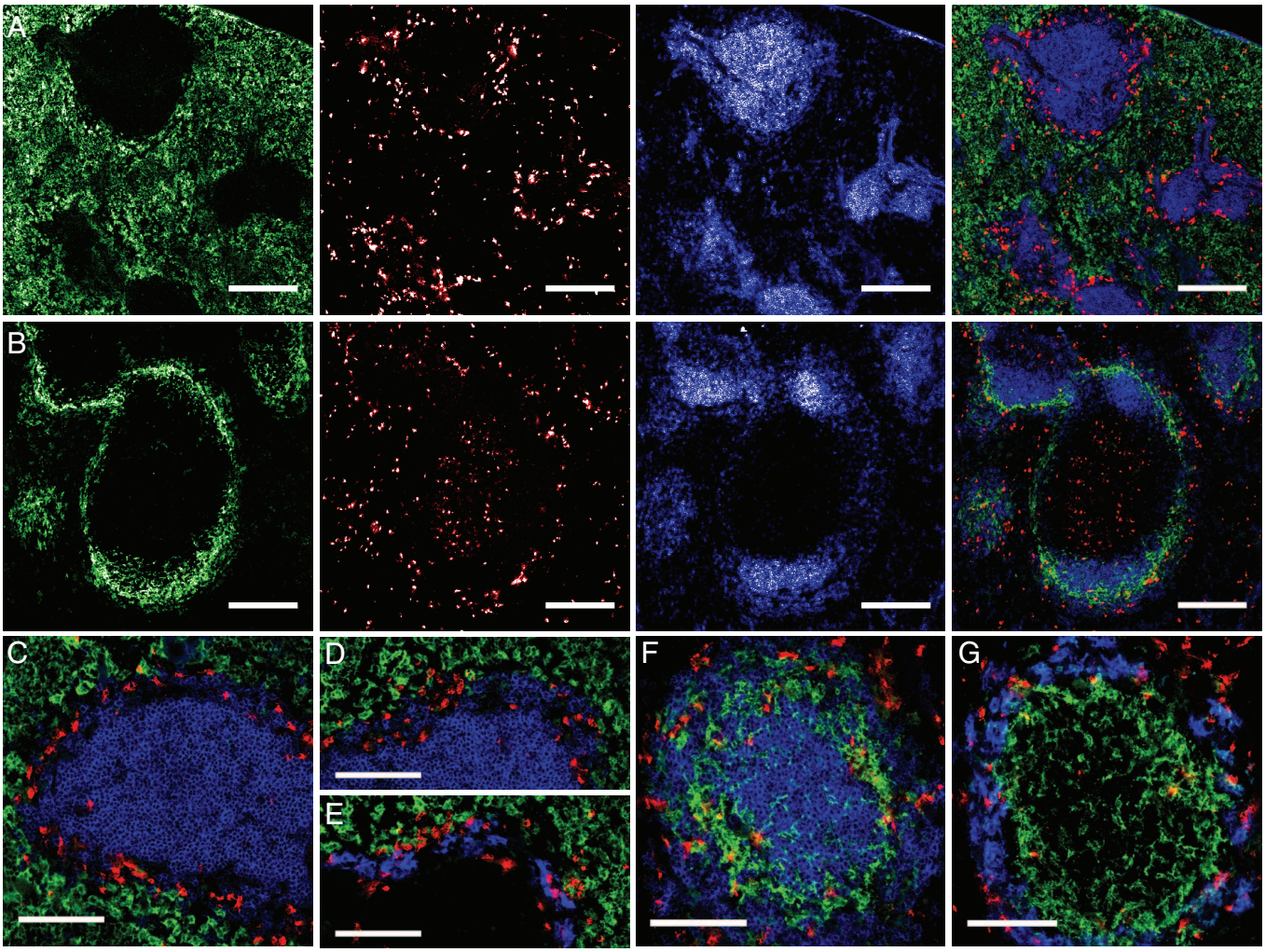

Fig. 2. Langerin$^+$ cells predominate in the MZ and are distinct from macrophages. (*A* and *B*) Splenic sections of BALB/c mice were stained in green for F4/80 (*A*) or CD169 (*B*), red for Langerin, and blue for B220. (Scale bar: 200 μm.) (*C–G*) Higher magnification of splenic RP and MZ with Langerin$^+$ cells in red. RPMs were stained with F4/80 (*C–E*, green), MMMs with CD169 (*F* and *G*, green), and MZMs with SIGNR1 (*E* and *G*, blue). B220 (blue) delineates WP in *C*, *D*, and *F*. (Scale bar: 100 μm.)

were not labeled with fluorescent particles (Fig. 5*A*). Likewise, CD11c$^+$ and CD8$^+$ MZ DCs rarely contained particles (Fig. 5*B*; lower magnifications are in Fig. S2). In contrast, uptake of YG-PS by RPMs, MMMs, and MZMs was readily evident (Fig. 5*C* and Fig. S3).

Similar results were obtained when the uptake of fluorescent killed *E. coli* and *S. aureus* was analyzed by tissue sections. Langerin$^+$ cells were rarely labeled with fluorescent bacteria (Fig. 5 *D* and *E Left*), whereas RPMs and particularly MMMs took up numerous fluorescent particles (Fig. 5 *D* and *E Center* and *Right*). When subsequent time points were examined (e.g., 3 h), only a few cells with fluorescent *E. coli* and *S. aureus* were found, indicating that particles were actively digested (data not shown), but the indigestible YG-PS particles persisted at least 48 h (the longest time point studied), again in MZ and RP macrophages, not Langerin$^+$ DCs. Thus, the bulk of particle clearance from the blood is by macrophages, not DCs, even though both cell types are juxtaposed in situ.

Microbial Agonists Induce Marked Changes in the Localization of Langerin. Previously, De Smedt *et al.* (19) reported that systemic inoculation of LPS led to a redistribution of CD11c$^+$ DCs from the MZ to the T cell area, whereupon the cells disappeared. To determine the response to microbial agonists, we injected either poly(IC) (Fig. 6) or LPS (Fig. S4*A*), the former a mimic for double-stranded RNA and the latter a constituent of bacterial cell walls. In the absence of microbial mimics, YG-PS beads remained mainly in the MZ and RP (Fig. 6 and Fig. S4*A Left*), and only a few particles were in WP, even 48 h after particle injection (data not shown). Likewise, Langerin$^+$ cells remained primarily in the MZ after particle injection (Fig. 6 and Fig. S4*A Left*). However, poly(IC) (Fig. 6) or LPS (Fig. S4*A*), which induced the phenotypic maturation of CD8$^+$ DCs during the first 12 h (Fig. S4*B*), led to a marked loss of Langerin from the MZ and RP, whereas Langerin staining in PALS increased markedly (Fig. 6 and Fig. S4*A Middle*); some cells in the PALS contained single latex particles, consistent with transport by Langerin$^+$ cells from the MZ (Fig. 6 *Center*, arrowhead). By 48 h, Langerin staining had disappeared (Fig. 6 and Fig. S4*A Right*). Further studies will be required to determine whether these marked changes in Langerin expression reflect movement of Langerin$^+$ cells from MZ into PALS and then cell death.

Discussion

Our findings have used a new IgG anti-Langerin/CD207 mAb (23) to visualize CD8$^+$ DCs more clearly than previously pos-

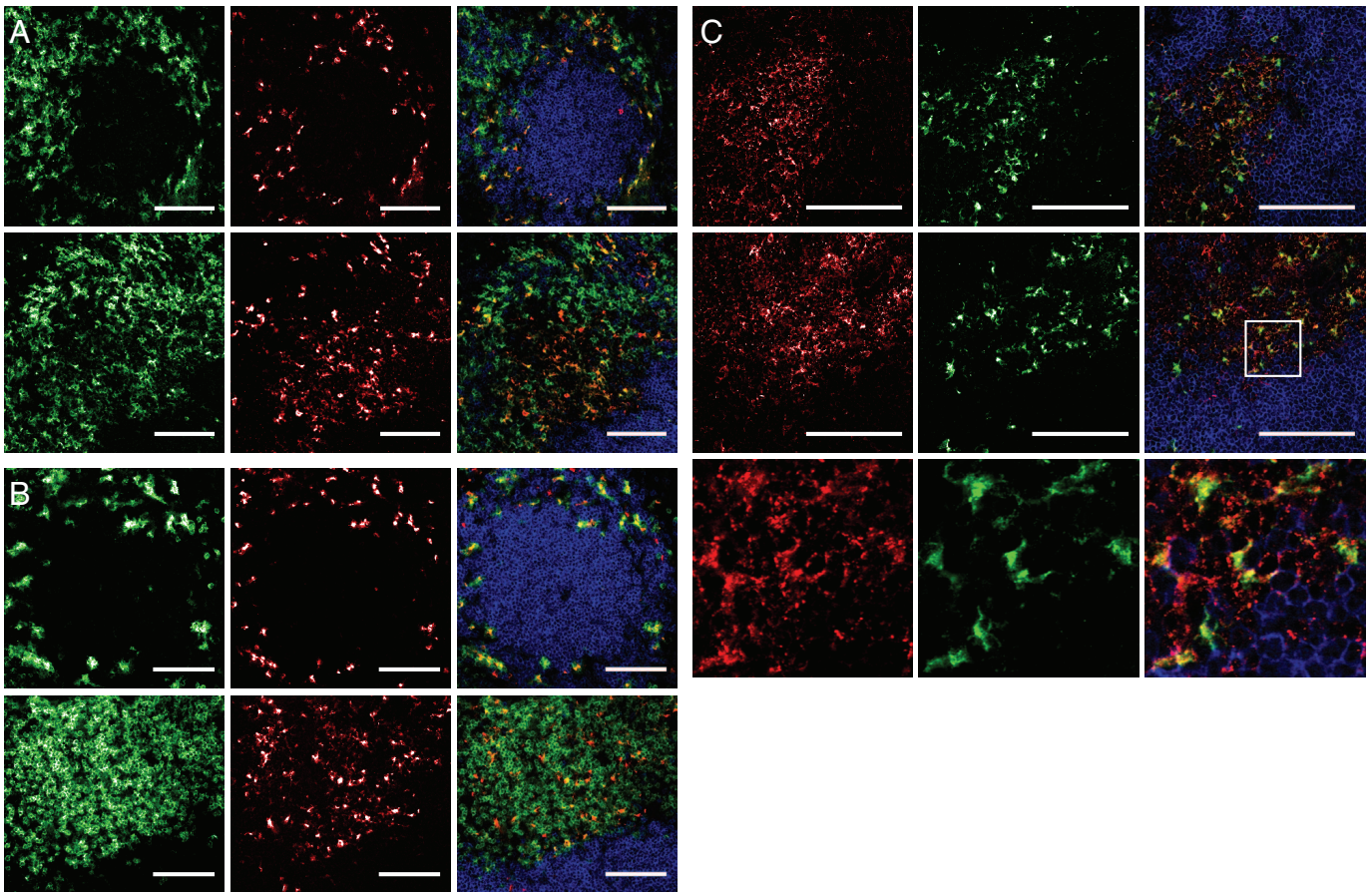

Fig. 3. L31 anti-Langerin mAb localizes most CD8α^+ DCs to the MZ. (*A*) BALB/c spleen sections were stained for CD11c (green), Langerin (red), and B220 (blue). Langerin$^+$ CD11c$^+$ cells in the MZ (*Upper*) and T cell area (*Lower*). (*B*) CD8$^+$ DCs (green) costained for Langerin (red) in the MZ (*Upper*) and T cell area (*Lower*). (*C*) Cryosections were stained for DEC205 (red), Langerin (green), and B220 (blue). (*Bottom*) Magnified region of *Middle* (white square). (Scale bar: 100 μm.)

sible. This subset of CD11c^{high} DCs labels for CD8, CD205, and CD207/Langerin by FACS but, relative to other markers, Langerin appears to be superior for localization studies in sections. CD8 and CD207 are clearly coexpressed on the same cells in the MZ, but in the T cell area and RP CD207 is a better marker because of abundant expression of CD8 on adjacent CD207$^-$ T cells. Likewise, CD205 is currently a relatively weak marker for tissue section staining, and it primarily labels cells in the T cell area rather than the MZ. The drawback of Langerin is that it is not expressed strongly on CD8$^+$ DCs in C57BL/6 mice (23, 30).

Our findings with CD207 impinge on 2 aspects of mouse spleen function, the major organ for immunological studies in this species. The first relates to the localization of CD8$^+$ DCs. Previously, splenic CD8$^+$ DCs were thought to be localized to

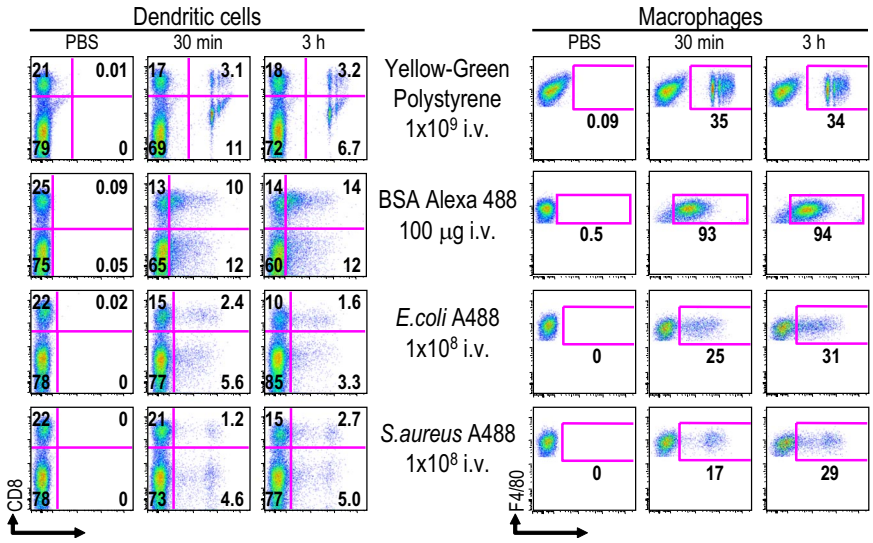

Fig. 4. Weak phagocytosis of bloodborne substrates by Langerin$^+$ CD8$^+$ marginal zone DCs. Pseudodot plots of CD19-depleted splenocytes 30 min or 3 h after injecting BALB/c mice with PBS or different substrates, indicated in the center as follows: YG-PS, BSA, *E. coli*, or *S. aureus*. Dendritic cell (CD11c^{hi}) phagocytosis was assessed in CD8$^+$ and CD8$^-$ subsets (Fig. S1, gate g); also, the uptake of bloodborne particles by red pulp macrophages (Fig. S1, gate j) was evaluated.

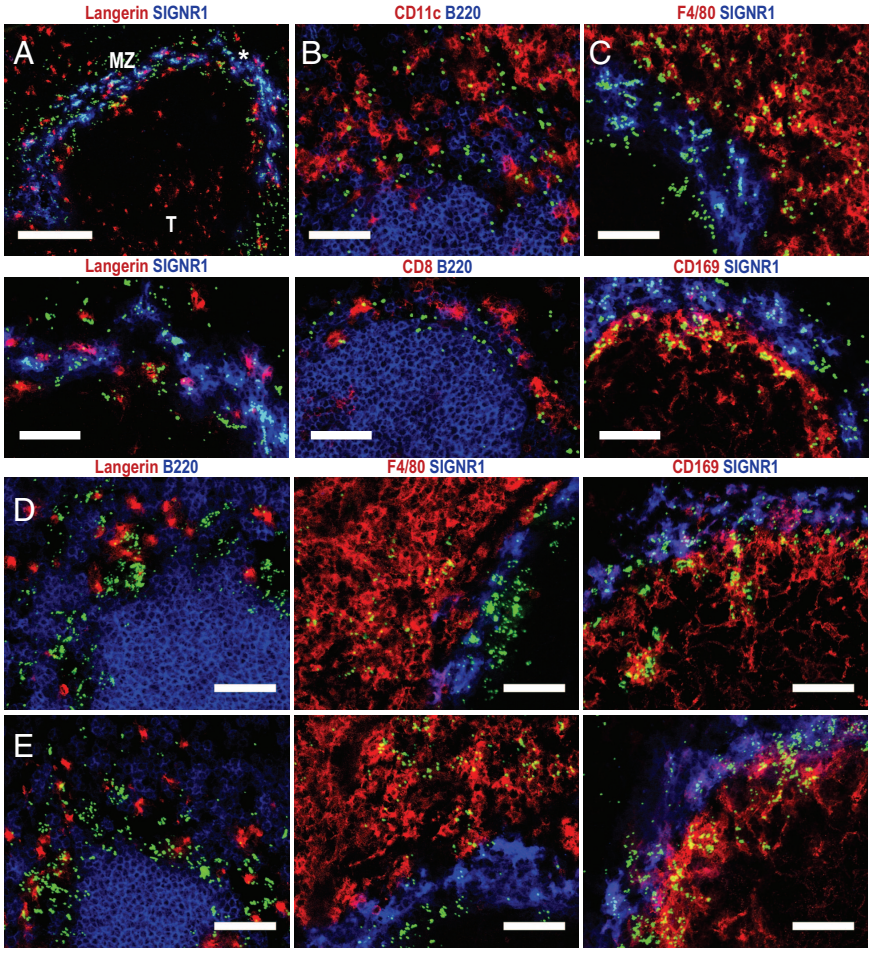

Fig. 5. Polystyrene, *E. coli*, and *S. aureus* accumulate in RP and MZ macrophages but not Langerin$^+$ cells. (*A*) Cryosections of spleen were examined 30 min after the injection of YG-PS. In addition to the green YG-PS, primarily in the MZ, sections were stained with L31 mAb, followed by Alexa 555 anti-rat Ig (red) and Alexa 647 SIGNR1 (blue). (*Lower*) Magnified region of *Upper* (*). MZ indicates marginal zone; T, T cell area. (Scale bar: *Upper*, 150 μm; *Lower*, 100 μm.) (*B*) As in *A*, but sections were stained with α-CD11c (*Upper*, red) or α-CD8 (*Lower*, red) and Alexa 647 B220 (blue). (Scale bar: 100 μm.) (*C*) As in *A*, but sections were stained with α-F4/80 (*Upper*, red) or α-CD169 (*Lower*, red) and Alexa 647 α-SIGNR1 (blue). (Scale bar: 100 μm.) (*D* and *E*) Mice were inoculated with Alexa 488-labeled *E. coli* (*D*) or *S. aureus* (*E*) i.v. for 30 min. Sections were stained with α-Langerin (*Left*, red), α-F4/80 (*Center*, red), or α-CD169 (*Right*, red), and Alexa 647-B220 (*Left*, blue) or SIGNR1 (*Center* and *Right*, blue). (Scale bar: 100 μm.)

DEC205-rich T cell areas (20–22). However, we found that large numbers of CD8$^+$ CD207$^+$ CD11c$^+$ DCs are localized in the MZ, with smaller numbers in RP and PALS. Previously, few CD8$^+$ DC have been localized in the MZ (12, 31), and some CD8$^+$ DCs are involved in the early uptake of *Listeria monocytogenes* (32) and dying cells (33) injected i.v. Production of large amounts of IL-12 is also a distinct feature of CD8$^+$ DCs (34), and in situ analysis after injection of *Toxoplasma gondii* extracts localized IL-12 production in the MZ (35). Nevertheless, we found that CD207$^+$ MZ and RP DCs are readily distinguished by molecular markers from the different populations of macrophages in these regions (i.e., F4/80$^+$ RPM, SIGNR1$^+$ MZM, and CD169$^+$ MMM cells). Our findings apply to the steady state. Upon microbial stimulation, CD207 expression changes markedly, first increasing in the PALS and then disappearing, implying movement of the corresponding cells to the PALS, followed by their loss.

The second aspect of spleen function relates to the MZ and RP as regions specialized for particle clearance from the blood (16, 17). Small vessels empty into the MZ (17) so that large blood-borne particles gain access to phagocytes and seem precluded to enter directly to the WP (36). Langerin$^+$ CD8$^+$ DCs are therefore ideally placed to have access to particles trapped in the MZ. Nevertheless, using polystyrene particles or bacteria, little uptake was evident in CD207$^+$ DCs, whereas uptake in MZ phagocytes was much stronger, particularly when tissue sections

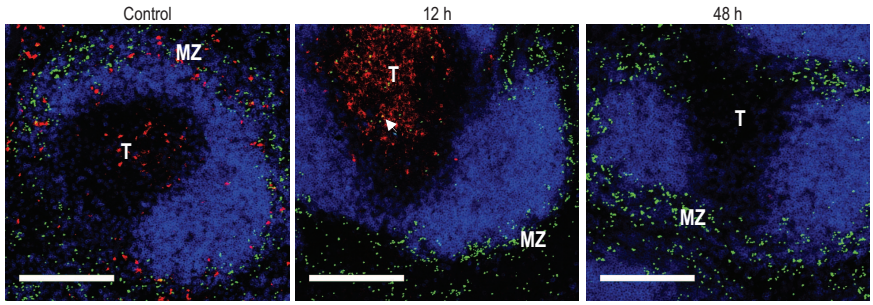

Fig. 6. Poly(IC) induces marked changes in Langerin expression. BALB/c mice were injected i.v. with YG-PS 30 min before inoculation of PBS (*Left*) or 50 μg of poly(IC) i.p (*Center* and *Right*). At 12 h (*Left* and *Center*) or 48 h (*Right*) later, spleen sections were stained with L31 mAb, followed by Alexa 555 anti-rat Ig (red) and Alexa 647 anti-B220 (blue). MZ indicates marginal zone; T, T cell area. (Scale bar: 200 μm.)

were examined. Previously, it had been reported and we confirmed that $CD8^+$ DCs take up dying cells (33), so different populations of cells in the MZ and RP must express different receptors for phagocytic uptake.

Our findings change the view of $CD8^+$ DCs as a subset that has a major representation in the MZ, not just the T cell area, and thus is positioned to capture bloodborne antigens. The assays we used in this study primarily assess the level of particle scavenging or clearance, a feature of macrophages, but do not allow an assessment of the low levels of uptake that suffice for antigen processing and presentation by DCs to T cells.

Materials and Methods

Mice. BALB/c mice (Harlan Sprague–Dawley) were maintained under specific pathogen-free conditions. Animal care and experiments were conducted according to the institutional guidelines of The Rockefeller University.

Reagents. All fluorochrome-labeled mAbs are listed in Table S1. α-Langerin (L31) (23), α-DCIR2 (33D1) (10), α-DEC205 (NLDC145) (13, 14), and α-OLLAS tag (37) were produced in house, purified on protein G (Pierce), and labeled with Alexa 647 (Invitrogen) or EZ-Link Biotin (Pierce) per the manufacturer's instructions. Other reagents were LIVE/DEAD Fixable Aqua Stain (Invitrogen), DAPI (Sigma–Aldrich), poly(IC) (InvivoGen), and LPS (*E. coli* serotype 055:B5; Sigma–Aldrich).

Cell Preparation and Flow Cytometry. Spleens were digested 25 min at 37 °C in Hanks buffer (Gibco) with 400 units/mL Collagenase D (Roche) and 50 μg/mL DNaseI (Roche). A total of 5 mM EDTA (Gibco) was added for the last 5 min. Red blood cells were lysed (BioWhittaker), and samples were passed through a nylon mesh to remove undigested material. The cells were B cell-depleted with α-CD19 magnetic beads and passed through LS columns (Miltenyi Biotec). For flow cytometry, nonspecific binding was first blocked with 2.4G2 supernatant anti-FcR II/III, and then cells were stained at 4 °C in PBS/2% FBS (FACS buffer). For intracellular staining, cells were washed with PBS, stained with LIVE/DEAD Fixable Aqua, and fixed/permed with Cytofix/Cytoperm solution (BD Biosciences). Cells were stained with different cocktails of mAbs and gated as shown in Fig. S1. Multiparameter acquisition was done on an LSR II (Becton Dickinson), followed by analysis with FlowJo (TreeStar).

In Vivo Delivery of Fluorescent Particles. We injected i.v. 100 μL of 0.27% 1-μm Fluoresbrite Yellow Green Carboxylate Microspheres (YG-PS; Polysciences Inc.), 10^8 inactivated *E. coli* Alexa 488 (Invitrogen), 10^8 *S. aureus* Alexa 488 (Invitrogen), or 100 μg of BSA Alexa 488 (Invitrogen).

Fluorescence Microscopy. Spleens were frozen in optimal cutting temperature compound (Tissue-Tek OCT; Sakura), sectioned at 10–15 μm, fixed 15 min in cold acetone, rehydrated in PBS, and blocked first with Avidin/Biotin Blocking reagents (Zymed), followed by blocking with 5% mouse serum in FACS buffer for 1 h at room temperature. Sections were stained in a humidified chamber overnight at 4 °C with primary mAbs (Table S2), washed in FACS buffer, and stained 1 h at room temperature with secondary mAbs. If necessary, sections were incubated with 5% rat serum to block free arms of secondary mAbs, and were stained with fluorochrome-labeled third mAbs (Table S2). DEC205 staining used α-DEC205-OLLAS-OVA as described previously (15, 37). Sections were mounted in Aqua-Poly Mount (Polysciences Inc.), examined in a Zeiss LSM 510 system (Carl Zeiss Inc.) at the Rockefeller University Bio-Imaging Resource Center, and analyzed with ImageJ (National Institutes of Health).

ACKNOWLEDGMENTS. We thank Dr. K. Inaba (Kyoto University, Kyoto, Japan) for discussions; J. Adams and A. Gottfried for preparing figures; J. Kuroiwa for technical support; and S. Mazel and A. North (The Rockefeller University Flow Cytometry and Bio-imaging Resource Centers). This work was supported by National Institutes of Health Grants AI13013 and AI51573 (to R.M.S.), and the Gates Foundation Centers for AIDS Vaccine Discovery.

1. Pulendran B, Palucka K, Banchereau J (2001) Sensing pathogens and tuning immune responses. *Science* 293:253–256.
2. Steinman RM (2008) Dendritic cells in vivo: A key target for a new vaccine science. *Immunity* 29:319–324.
3. Shortman K, Naik SH (2007) Steady-state and inflammatory dendritic-cell development. *Nat Rev Immunol* 7:19–30.
4. Villadangos JA, Schnorrer P (2007) Intrinsic and cooperative antigen-presenting functions of dendritic-cell subsets *in vivo*. *Nat Rev Immunol* 7:543–555.
5. Vremec D, Pooley J, Hochrein H, Wu L, Shortman K (2000) CD4 and CD8 expression by dendritic cell subtypes in mouse thymus and spleen. *J Immunol* 164:2978–2986.
6. den Haan JM, Lehar SM, Bevan MJ (2000) $CD8^+$ but not $CD8^-$ dendritic cells cross-prime cytotoxic T cells in vivo. *J Exp Med* 192:1685–1696.
7. Maldonado-Lopez R, *et al.* (1999) $CD8a^+$ and $CD8\alpha^-$ subclasses of dendritic cells direct the development of distinct T helper cells in vivo. *J Exp Med* 189:587–592.
8. Pulendran B, *et al.* (1999) Distinct dendritic cell subsets differentially regulate the class of immune responses *in vivo*. *Proc Natl Acad Sci USA* 96:1036–1041.
9. Soares H, *et al.* (2007) A subset of dendritic cells induces $CD4^+$ T cells to produce IFN-γ by an IL-12-independent but CD70-dependent mechanism in vivo. *J Exp Med* 204:1095–1106.
10. Dudziak D, *et al.* (2007) Differential antigen processing by dendritic cell subsets *in vivo*. *Science* 315:107–111.
11. Schnorrer P, *et al.* (2006) The dominant role of $CD8^+$ dendritic cells in cross-presentation is not dictated by antigen capture. *Proc Natl Acad Sci USA* 103:10729–10734.
12. McLellan AD, *et al.* (2002) Anatomic location and T-cell stimulatory functions of mouse dendritic cell subsets defined by CD4 and CD8 expression. *Blood* 99:2084–2093.
13. Kraal G, Breel M, Janse M, Bruin G (1986) Langerhans cells, veiled cells, and interdigitating cells in the mouse recognized by a monoclonal antibody. *J Exp Med* 163:981–997.
14. Jiang W, *et al.* (1995) The receptor DEC-205 expressed by dendritic cells and thymic epithelial cells is involved in antigen processing. *Nature* 375:151–155.
15. Idoyaga J, *et al.* (2008) Langerin/CD207 receptor on dendritic cells mediates efficient antigen presentation on MHC I and II products in vivo. *J Immunol* 180:3647–3650.
16. Kraal G (1992) Cells in the marginal zone of the spleen. *Int Rev Cytol* 132:31–74.
17. Mebius RE, Kraal G (2005) Structure and function of the spleen. *Nat Rev Immunol* 5:606–616.
18. Steinman RM, Pack M, Inaba K (1997) Dendritic cells in the T cell areas of lymphoid organs. *Immunol Rev* 156:25–37.
19. De Smedt T, *et al.* (1996) Regulation of dendritic cell numbers and maturation by lipopolysaccharide in vivo. *J Exp Med* 184:1413–1424.
20. Naik SH (2008) Demystifying the development of dendritic cell subtypes, a little. *Immunol Cell Biol* 86:439–452.
21. Lopez-Bravo M, Ardavin C (2008) In vivo induction of immune responses to pathogens by conventional dendritic cells. *Immunity* 29:343–351.
22. Wu L, Liu YJ (2007) Development of dendritic-cell lineages. *Immunity* 26:741–750.
23. Cheong C, *et al.* (2007) Production of monoclonal antibodies that recognize the extracellular domain of mouse Langerin/CD207. *J Immunol Methods* 324:48–62.
24. Douillard P, *et al.* (2005) Mouse lymphoid tissue contains distinct subsets of langerin/CD207 dendritic cells, only one of which represents epidermal-derived Langerhans cells. *J Invest Dermatol* 125:983–994.
25. Taylor PR, *et al.* (2005) Macrophage receptors and immune recognition. *Annu Rev Immunol* 23:901–944.
26. Inaba K, *et al.* (1995) Tissue distribution of the DEC-205 protein that is detected by the monoclonal antibody NLDC-145. I. Expression on dendritic cells and other subsets of mouse leukocytes. *Cell Immunol* 163:148–156.
27. Kronin V, Wu L, Gong S, Nussenzweig MC, Shortman K (2000) DEC-205 as a marker of dendritic cells with regulatory effects on CD8 T cell responses. *Int Immunol* 12:731–735.
28. Witmer-Pack MD, Swiggard WJ, Mirza A, Inaba K, Steinman RM (1995) Tissue distribution of the DEC-205 protein that is detected by the monoclonal antibody NLDC-145. II. Expression in situ in lymphoid and nonlymphoid tissues. *Cell Immunol* 163:157–162.
29. Valladeau J, *et al.* (2000) Langerin, a novel C-type lectin specific to Langerhans cells, is an endocytic receptor that induces the formation of Birbeck granules. *Immunity* 12:71–81.
30. Flacher V, *et al.* (2008) Expression of Langerin/CD207 reveals dendritic cell heterogeneity between inbred mouse strains. *Immunology* 123:339–347.
31. Fazekas De St Groth B, *et al.* (2002) Experimental models linking dendritic cell lineage, phenotype and function. *Immunol Cell Biol* 80:469–476.
32. Neuenhahn M, Busch DH (2007) Unique functions of splenic $CD8\alpha^+$ dendritic cells during infection with intracellular pathogens. *Immunol Lett* 114:66–72.
33. Iyoda T, *et al.* (2002) The $CD8^+$ dendritic cell subset selectively endocytoses dying cells in culture and in vivo. *J Exp Med* 195:1289–1302.
34. Hochrein H, *et al.* (2001) Differential production of IL-12, IFN-α, and IFN-γ by mouse dendritic cell subsets. *J Immunol* 166:5448–5455.
35. Reis e Sousa C, *et al.* (1997) In vivo microbial stimulation induces rapid CD40L-independent production of IL-12 by dendritic cells and their re-distribution to T cell areas. *J Exp Med* 186:1819–1829.
36. Nolte MA, *et al.* (2003) A conduit system distributes chemokines and small blood-borne molecules through the splenic white pulp. *J Exp Med* 198:505–512.
37. Park SH, *et al.* (2008) Generation and application of new rat monoclonal antibodies against synthetic FLAG and OLLAS tags for improved immunodetection. *J Immunol Methods* 331:27–38.